

System Analysis of a Programmed Cell Death Model

Eric Bullinger

Hamilton Institute, National University of Ireland Maynooth, Maynooth, Co. Kildare, Ireland

Abstract—Apoptosis is a programmed cell death by which the organism removes unwanted cells. Its core reactions can be described by a system of differential equations exhibiting multiple steady-states. In this paper we analyse how this model can include both very slow dynamics for the lag phase before apoptosis (in theory up to several days) while the apoptosis itself is more switch-like with changes occurring within minutes. We both describe how the trajectories evolve during the lag phase and show which of the states have the most impact on the slow dynamics.

I. INTRODUCTION

Apoptosis is a major form of programmed cell death enabling the organism to remove unwanted cells without harming their neighbours. This is important during embryonal development, after immune responses and to eliminate virally infected or transformed cells [8, 10]. A misregulation is implicated in severe pathological alterations, including developmental defects, auto-immune diseases, neurodegeneration or cancer. An in-depth understanding of the underlying mechanism is therefore of great medical interest.

Apoptosis is one of many signalling networks involved in the regulation of cells. These signals correspond to the presence or absence of specific molecules, often called messengers. Often, their presence alone does not contain all the information. Signal properties, but this is contained for example in the duration of the messenger's presence or the shape of the signal, see for example [4, 12] and is in particular the case for apoptotic signalling [11]. Another particularity often present in signalling networks are nonlinear phenomena such as multiple steady-states. A particular case is when two asymptotically stable steady-states exist in the attainable state space. This is called "bistability" and seems to be a key property of many switch-like phenomena like apoptosis or cell cycle regulation, see e.g. [1, 7, 9, 13, 15].

Finding the steady-states is only part of understanding these systems. As timing and type of transient behaviour might characterise the actual information of the signalling network, system theoretical analysis methods play a key role helping to explain both the attainable behaviour of a model as well as its sensitivity with respect to changes of the parameters, see2 e.g. [2, 3, 16].

In this paper, we analyse a model of apoptosis to understand why it exhibits long lag phases of up to several days, even though the output changes significantly only within a few minutes.

E. Bullinger is also with the Institute for Systems Theory in Engineering, University of Stuttgart, 70550 Stuttgart, Germany. eric.bullinger@nuim.ie

II. MODEL

A model of the core of apoptosis decision taking has been proposed by [6]. It considers the mutual activation of caspase 8 (C8) and 3 (C3) constituting a positive feedback loop. Activated caspase 3 (C3*) serves as an output and is inhibited by inhibitor of apoptosis (IAP) proteins. Activated caspase 8 (C8*) serves as an input and is inhibited by CARP, see Figure 1. The corresponding reactions can be found in R1 to R13.

This model does not include how caspase 8 is activated. It is for example not known how many receptors need to be active for enabling a signal leading to activation of caspase 8, or whether this is only possible via sufficiently large clusters of the receptors, see for example [14, 17]. Also, the signal form of the receptor induced activation of caspase 8 is not known. In this study, as in [6], we analyse impulse responses, which is equivalent to starting with a certain amount of activated caspase 8 (C8*) at time zero.

The output of the model, activated caspase 3 (C3*) is the active form of an effector caspase which cleave essential proteins, quickly leading to the break-up of the cell without harming its environment.

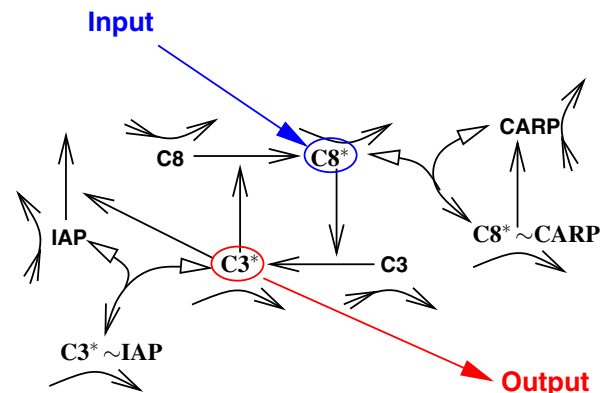
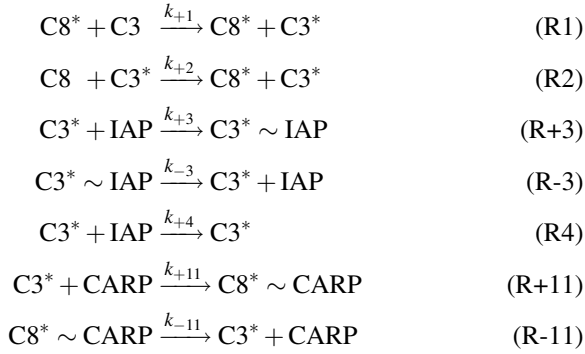
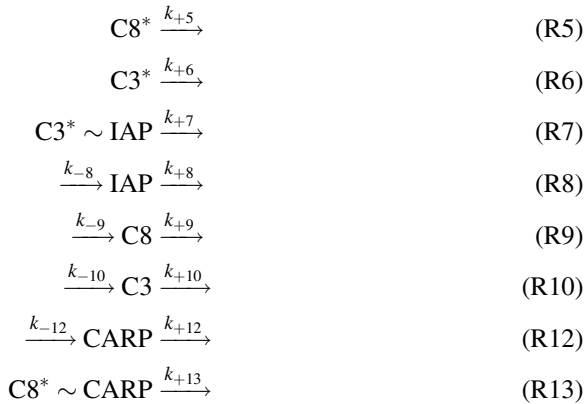


Fig. 1. Reaction scheme of the apoptosis model. Reactions are depicted by arrows. The triangular arrows depict the backwards part of reversible reactions. All molecules are also degraded and C8, C3, IAP and CARP are also produced, depicted by the arrows close the corresponding components.



plus eight turnover reactions:



All reactions are modelled according to the law of mass action. Therefore, a reaction $A + B \xrightarrow{k} C$ corresponds to a flux of $v = k \cdot A \cdot B$ which is added to the mass balance of C , subtracted from the ones of A and B . Equivalently, reactions for (external) production are modelled as $\xrightarrow{k} A$, corresponding to a flux of $v = k$ while reactions for degradation are modelled as $A \xrightarrow{k}$, corresponding to a flux of $v = k \cdot A$.

Summarising, the system has 8 states, and 13 reaction, of which 6 are bidirectional and therefore 19 parameters, see Table I. Due to Reactions (R1) to (R4) and (R11), the system is nonlinear. As the states represent concentrations, for the state space only the positive orthant is of interest.

TABLE I
PARAMETERS (ALL IN MIN^{-1}).

$k_{+1} = 5.8\text{e-}5$	$k_{+11} = 0.0005$
$k_{+2} = 1.0\text{e-}5$	$k_{+12} = 0.001$
$k_{+3} = 0.0005$	$k_{+13} = 0.0116$
$k_{+4} = 0.0003$	$k_{-3} = 0.21$
$k_{+5} = 0.0058$	$k_{-8} = 464$
$k_{+6} = 0.0058$	$k_{-9} = 507$
$k_{+7} = 0.0173$	$k_{-10} = 81.9$
$k_{+8} = 0.0116$	$k_{-11} = 0.21$
$k_{+9} = 0.0039$	$k_{-12} = 40$
$k_{+10} = 0.0039$	

The system has three steady-states in the closed positive orthant, which is the domain of interest for states representing concentrations, see Table II. Steady-state 1 has no active caspases present and corresponds to the life condition. This steady-state will also serve as initial condition for the simulations, except for C8^* whose value will depend on the strength of the impulse used as input. The second equilibrium is a saddle with a one-dimensional unstable manifold. The third steady-state corresponds to high levels of active caspases and to apoptosis.

TABLE II
STEADY STATES OF THE SYSTEM (ALL IN MOLECULES PER CELL).

State	SS1	SS2	SS3
C8	130000	129869.00	9132.37
C8^*	0	0.49	74380.10
C3	21000	20847.50	18.97
C3^*	0	0.39	5161.68
IAP	40000	39546.40	264.16
$\text{C3}^* \sim \text{IAP}$	0	34.24	2999.32
CARP	40000	39491.70	20.54
$\text{C8}^* \sim \text{CARP}$	0	43.82	3446.51

The key property of the systems is the following: The system is in the life steady-state for negative times and at time zero, an impulse input activates a certain number of caspase 8. Below an impulse input of 75 molecules/cell of C8^* , the trajectories return to the life steady-state. Above this threshold, the states stay for a relatively long time in a vicinity of the life steady-state and then quickly move to the other stable equilibrium. For example, with an input of 1000 molecules/cell of C8^* , the transition takes place after about 16h. As shown in Figure 2, the increase of C3^* , the system output and trigger to apoptosis, is taking place within a few minutes.

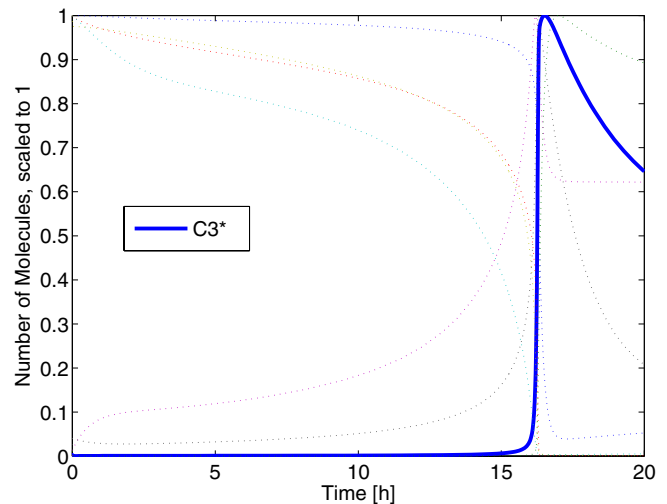


Fig. 2. Time course of the states, scaled by their maximal values for an input of 1000 molecules/cell of C8^* .

Analysing where this lag phase is “encoded” in the sys-

tem's equation is the objective of this paper. The concentration of the proteins, in particular of the inhibitors CARP and CARP, significantly influences the system behaviour. The analysis of the interplay between different input strength and amount of inhibitors in the topic of current study.

III. RESULTS

The saddle equilibrium has a one-dimensional unstable manifold connecting all three steady-states. Starting close to the saddle on the on this manifold, it takes about 45 days for reaching the steady-state corresponding to apoptosis taking place. This is much longer than the time frame the model is assumed to be valid in as for example changes in the gene expression level can easily take place during this time span. It is reasonable to assume that either apoptosis occurs within two days after a stimulation, or none will occur. 48h corresponds to an initial C8 activation of about 350 molecules per cell. Thus, the interval between 75 and 350 molecules per cell might be interesting for a system analysis but the model prediction is biologically not relevant.

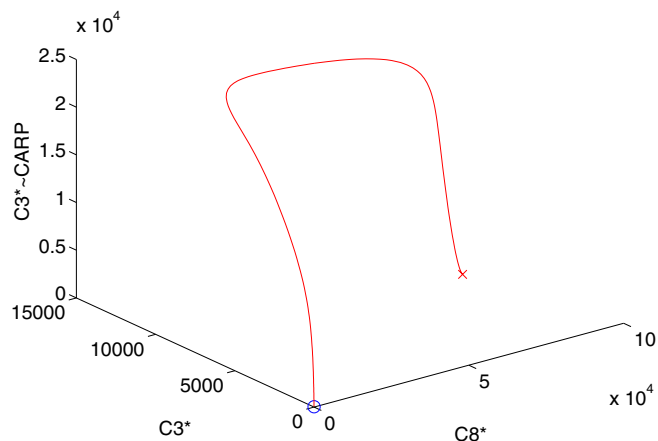


Fig. 3. Unstable Manifold. Steady-state 3: x, steady-states 1 and 2: o. In this projection, the first two steady-states are not discernible.

An interesting feature of the model is that the trajectories seem to converge to the unstable manifold. Figure 4 shows how trajectories approach the unstable manifold for different values of initial $C8^*$, below the critical value of 75 molecules/cell. Figure 5 shows a similar behaviour for trajectories leading to apoptosis.

Figure 6 shows the whole trajectories leading to apoptosis. Close to the origin, the trajectories differ, see also Figure 5. Then, they are very close to each other in this projection and only for very large $C3^*$ is a difference again visible. The middle part is precisely the lag phase in which the trajectories spend several hours.

The number of active caspases is very low up to the start of the apoptosis. For example in Figure 4, there are at most two molecules per cell of $C3^*$. This means that stochastic simulations should be used as has been done in [5] showing that the stochastic effects are important for low level of initial input. The boundary between apoptosis and survival is also

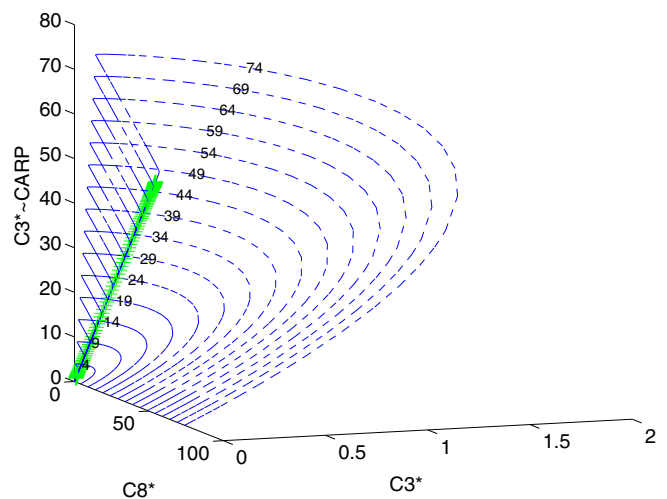


Fig. 4. Heterocline between saddle and life steady-state (green plus signs) together with simulations corresponding to different levels of initial $C8^*$ (number on trajectory).

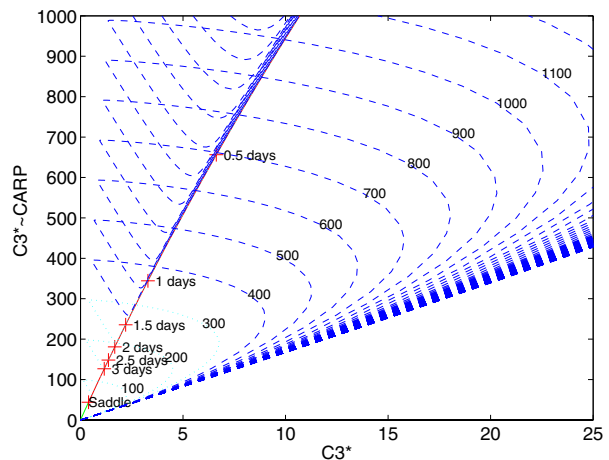


Fig. 5. Unstable manifold and trajectories yielding apoptosis (initial values of $C8^* = 100 : 100 : 5000$). On the manifold, the time until apoptosis is marked.

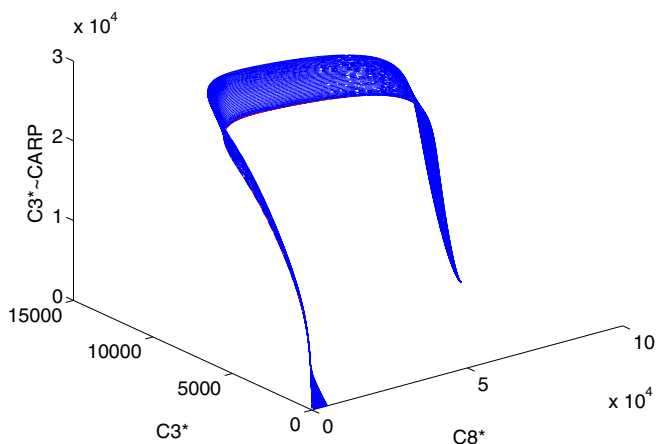


Fig. 6. Unstable manifold and trajectories yielding apoptosis (initial values of $C8^* = 100 : 100 : 5000$).

not sharp in the stochastic case. However, if apoptosis should happen within a biologically reasonable time, the system behaves relatively close to the deterministic case.

A. Quasi-steady-state Approximation

The life steady-state is the easiest steady-state to analyse as half of the states are zero. This allows to also get analytic solutions for four of the eight eigenvalues, see Table III. The eigenvalues are five orders of magnitude apart: $10e-4$ to $10e1$. The fastest two are related to the binding of active caspases to IAP or CARP. The eigenvector corresponding to the slowest eigenvalue is parallel to the heterocline from the saddle and is related to the total amount of bound caspases.

From this local analysis, one can conjecture that the free active caspases, $C8^*$ and $C3^*$, are in quasi-steady-state. The initial concentration of $C8^*$ is the input to the full system. This state is however eliminated in the reduced model. Therefore, as input of the reduced model, we start with $C8^*$ immediately in its bound form, namely $C8^*\text{-CARP}$. Simulations below the apoptosis threshold (Figure 7(a)) and above (Figure 7(b)) show that this is indeed not a bad approximation.

The quasi-steady-state approximation gives another explanation why stochastic effects can be neglected. While the number of free active caspases is very low, the number of bound ones is substantially higher. In stochastic simulations, the reactions between free and bound form occur very frequently, but do not significantly change the overall behaviour of the system.

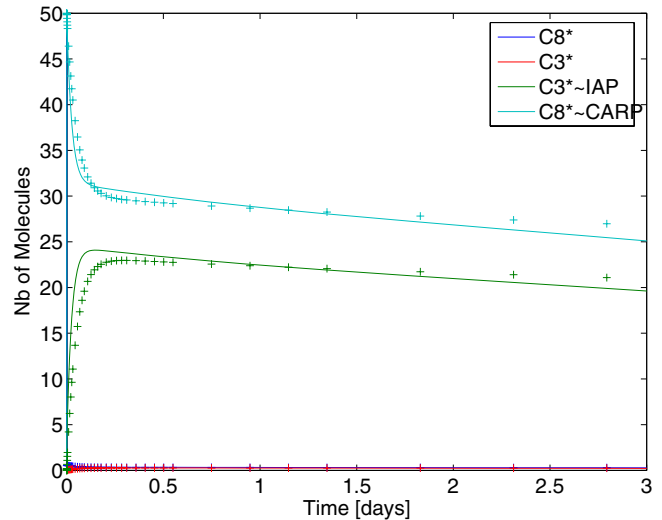
B. Analysis of the Lag-phase

Around the life steady-state, the slowest eigenvalue corresponds to the total amount of inhibitors IAP and CARP bound to their respective caspase. When simulating the lag phase, this is still a good approximation, see Figure 8. The rapid jump of the output, $C3^*$, is due to a related state, namely of CARP. Only when CARP is depleted, can there be a sufficient amount of free $C3^*$ to start the positive feedback loop: $C3^*$ activates C8 and $C8^*$ activates C3.

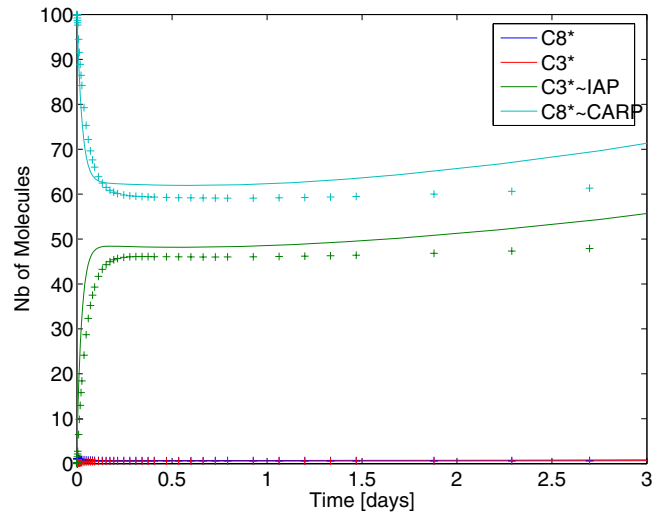
10h after a stimulus of 1000 $C8^*$, the relative change of the states is at most 0.6%, while the decrease of the inhibitors is negligible at a relative scale. The total decrease is however already perceptible, see Figure 8.

As shown above, the trajectory comes close to the saddle before slowly moving in the vicinity of the heterocline towards the death equilibrium. At the saddle, the eigenvalues are very close to the ones at the life steady-state, compare Tables IV with III. While the eigenvalues are still close, changes are visible in the corresponding eigenvectors. At the saddle, the fast dynamics are not dependent on the active caspases any more as also the free inhibitors appear in the corresponding modes. The slow modes are now dominated by the inhibitors, in particular by CARP, the inhibitor of the systems output $C3^*$.

At the 10h point discussed above, the eigenvalues are still in the same order of magnitude, see Table V. The fastest mode is now again hinting at a quasi-steady-state condition



(a) Initial concentration of $C8^*$ of 50.



(b) Initial concentration of $C8^*$ of 100.

Fig. 7. Simulation of the full system compared to a reduced-order model with quasi-steady-state assumptions for $C8^*$ and $C3^*$.

for IAP binding $C8^*$, while CARP remains important for the slowest mode.

IV. CONCLUSIONS AND FUTURE WORK

A. Conclusions

This paper analyses the dynamics of a model [6] describing the regulation of caspase, whose activation leads to programmed cell death, also called apoptosis. The model consists of 8 states evolving in the closed positive orthant. Within this subspace, three steady-states exist. One lies on the boundary, i.e. all activated caspases are zero, is asymptotically stable and corresponds to the life state. Another asymptotically stable steady state has large concentrations of active caspases and corresponds to the induction of programmed cell death. The third steady state is a saddle with a one-dimensional unstable manifold. This manifold is also the slow manifold of both stable steady-states.

TABLE III
EIGENVALUES (EV) AND EIGENVECTORS AT THE LIFE STEADY-STATE.

EV	exact	approx.	Mode
1		-21.46	$\approx + C8^* - C3^* + C3^*-IAP - C8^*-CARP$
2		-18.97	$\approx - C8^* - C3^* + C3^*-IAP + C8^*-CARP$
3		-0.02699	$\approx + C3^*-IAP - C8^*-CARP$
4	$-k_{+8}$	-0.0116,	IAP
5	$-k_{+9}$	-0.0039	C8
6	$-k_{+10}$	-0.0039,	C3
7	$-k_{+12}$	-0.001,	CARP
8		-0.000115	$\approx + C3^*-IAP + C8^*-CARP$

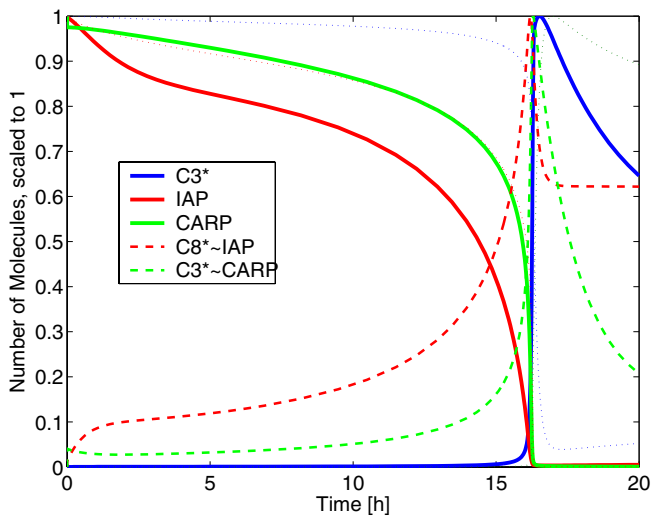


Fig. 8. Time course of the states, scaled by their maximal values for an input of 1000 molecules/cell of $C8^*$. The output, $C3^*$, quickly rises after both inhibitor, IAP and CARP, have been depleted.

For the life steady state, the slowest mode is approximately spanned by the sum of the two complex consisting of a caspase and its inhibitor. For the saddle as well as along the slow manifold between saddle and death steady state, the slow mode is dominated by the concentration of free CARP. This explains why a depletion of CARP corresponds to a significant mutual activation of caspases, a quick process towards the death steady state and to the programmed cell death.

Locally around the life steady state as well as along the slow manifold, the active caspases are in quasi-steady-state. This is a possible explanation why stochastic effects due to the low number of free caspases have a negligible effect on the system response [5].

B. Future Work

Having identified CARP as a key component of the lag phase behaviour, we would like to know how to best influence the length of the lag phase. This will be done via

TABLE IV
EIGENVALUES (EV) AND EIGENVECTORS AT THE SADDLE STEADY-STATE.

EV	approx.	Mode
1	-21.22	\approx all except C8 and C3
2	-18.74	\approx all except C8 and C3
3	-0.0270	\approx IAP
4	-0.0117	IAP
5	-0.0039	C8
6	-0.0039	C3 + C8
7	-0.001	\approx CARP + IAP
8	-0.00011	\approx CARP

TABLE V
EIGENVALUES (EV) AND EIGENVECTORS AFTER 10H, STARTING WITH $C8^*(0) = 1000$.

EV	approx.	Mode
1	-17.73	$\approx C8^* + IAP - C8^*-IAP$
2	-14.33	\approx IAP
3	-0.0274	\approx IAP
4	-0.0160	IAP
5	-0.0045	\approx IAP
6	-0.0040	\approx C8
7	-0.0032	\approx C8
8	-0.0020	\approx CARP

local as well as global sensitivity analyses.

V. ACKNOWLEDGEMENTS

The author gratefully acknowledge fruitful discussions with Thomas Eißing, Holger Conzelmann, Carla Cima- toribus, and Rolf Findeisen, all from the Systems Biology

Group at the University of Stuttgart, and very constructive comments for an anonymous reviewer.

REFERENCES

- [1] D. Angeli, J. E. J. Ferrell, and E. D. Sontag. Detection of Multi-stability, Bifurcations, and Hysteresis in a Large Class of Biological Positive-Feedback Systems. *Proc Natl Acad Sci U S A*, 101(7):1822–1827, 2004.
- [2] U. S. Bhalla. Robustness of the bistable behavior of a biological signaling feedback loop. *Chaos*, 11(1):221–226, 2001.
- [3] K.-H. Cho, S.-Y. Shin, W. Kolch, and O. Wolkenhauer. Experimental design in systems biology, based on parameter sensitivity analysis using a Monte Carlo method: A case study for the TNF α -mediated NF- κ B signal transduction pathway. *Simulation*, 79(12):726 – 739, 2003.
- [4] K.-H. Cho and O. Wolkenhauer. Analysis and Modelling of Signal Transduction Pathways in Systems Biology. *Biochem Soc Trans*, 31(6):1503–1509, 2003.
- [5] C. Cimadoribus, T. Eißing, N. Elvassore, F. Allgöwer, and E. Bullinger. Model discrimination in apoptosis. In *Foundations of Systems Biology FOSBE'05, Santa Barbara, CA, USA*, pages 197–200, 2005.
- [6] T. Eißing, H. Conzelmann, E. D. Gilles, F. Allgöwer, E. Bullinger, and P. Scheurich. Bistability analyses of a caspase activation model for receptor induced apoptosis. *J. Biological Chemistry*, 279(35):36892–36897, 2004.
- [7] J. Ferrell and W. Xiong. Bistability in Cell Signaling: How to Make Continuous Processes Discontinuous, and Reversible Processes Irreversible. *Chaos*, 11(1):227–236, 2001.
- [8] M. O. Hengartner. The biochemistry of apoptosis. *Nature*, 407:770–776, October 2000.
- [9] J. Keener and J. Sneyd. *Mathematical Physiology*, volume 8 of *Interdisciplinary Applied Mathematics*. Springer-Verlag, New York, second edition, 2001.
- [10] M. Leist and M. Jäättelä. Four deaths and a funeral: From caspases to alternative mechanisms. *Nature Reviews Molecular Cell Biology*, 2:589–598, 2001.
- [11] L. Marchetti, M. Klein, K. Schlett, K. Pfizenmaier, and U. L. M. Eisel. Tumor necrosis factor (TNF)-mediated neuroprotection against glutamate-induced excitotoxicity is enhanced by N-methyl-D-aspartate receptor activation. Essential role of a TNF receptor 2-mediated phosphatidylinositol 3-kinase-dependent NF- κ B pathway. *J Biol Chem*, 279(31):32869–32881, 2004.
- [12] C. J. Marshall. Specificity of receptor tyrosine kinase signaling: transient versus sustained extracellular signal-regulated kinase activation. *Cell*, 80(2):179–185, Jan 1995.
- [13] S. R. Neves and R. Iyengar. Modeling of Signaling Networks. *Bioessays*, 24(12):1110–1117, 2002.
- [14] D. Scheel-Toellner, K. Wang, L. K. Assi, P. R. Webb, R. M. Craddock, M. Salmon, and J. M. Lord. Clustering of death receptors in lipid rafts initiates neutrophil spontaneous apoptosis. *Biochem Soc Trans*, 32(5):679–681, 2004.
- [15] B. M. Slepchenko and M. Terasaki. Bio-switches: What Makes Them Robust? *Curr Opin Genet Dev*, 14(4):428–434, 2004.
- [16] J. Stelling, U. Sauer, Z. Szallasi, I. Francis J. Doyle, and J. Doyle. Robustness of cellular functions. *Cell*, 118:675–685, 2004.
- [17] G. Zhang. Tumor necrosis factor family ligand-receptor binding. *Curr Opin Struct Biol*, 14(2):154–160, 2004.